 doi:10.20944/preprints201908.0002.v1

Review

p53 Regulates Homeostasis in Irradiation-Injured Tissue in the Developing Brain and Mature Testis in the Small-Fish Model, Medaka (*Oryzias latipes*)

Takako Yasuda*

Department of Integrated Biosciences, Graduate School of Frontier Sciences, the University of Tokyo, Bioscience Bldg., Kashiwa, Chiba, 277-8562, Japan,

*Corresponding author: Department of Integrated Biosciences, Bioscience Bldg. 102, Kashiwa, Chiba 277-8562, Japan. tel: +81(0)471363663; fax: +81(0)471363669;

E-mail address: t_yasuda@edu.k.u-tokyo.ac.jp

Abstract

The tumor suppressor protein p53 is considered a guardian of genome integrity, regulating the induction of apoptosis and cell cycle arrest in response to irradiation to block the transmission of teratogenic mutations to progeny cells. We examined the function of p53 in highly radiosensitive tissues, the developing brain and mature testis, using a small fish model, medaka (*Oryzias latipes*). Medaka offer advantages as a vertebrate model system, as the transparency and small size of the

 doi:10.20944/preprints201908.0002.v1

embryos enables clear detection of apoptotic cells in the developing brain. In addition, the simple architecture of medaka testes enables more precise identification of the differentiating spermatogenic stages compared with mammals. We found that in irradiated p53-deficient embryonic brain, diminished induction of apoptosis facilitated tissue regeneration earlier compared to irradiated wild-type embryos, which remained structural abnormalities in the retina at hatching. Moreover, the prominent delay in apoptotic induction in irradiated p53-deficient testes could induce transient mis-differentiation during spermatogenesis, such as the formation of ovum-like cells (testis-ova). However, all testis-ova cells were eliminated via p53-independent apoptosis, and spermatogenesis was completely restored within 1 month after irradiation. Collectively, these data indicate that p53 is not indispensable for the restoration of irradiation-induced damaged tissues.

Keywords: p53, irradiation, medaka, developing brain, testis, apoptosis, regeneration, mis-differentiation

Introduction

The medaka (*Oryzias latipes*) is being used as a vertebrate model system in various fields of biology [1-4]. Medaka have also been used as an experimental animal model over the past few

Preprints (www.preprints.org) | NOT PEER-REVIEWED | Posted: 1 August 2019 doi:10.20944/preprints201908.0002.v1

decades to evaluate the biological effects of irradiation [5-9]. As an excellent vertebrate model for studying the developing central nervous system (CNS), small fish models such as medaka offer advantages over mouse models. For example, the transparency and small size of medaka embryos facilitates the detection of apoptotic neurons at the whole-brain level [6, 7]. In addition, compared with zebrafish, another popular laboratory fish model, the use of medaka enables more-precise observation of temporal changes in the apoptotic process after irradiation, as medaka morphogenesis is slower prior to hatching [10, 11]. Medaka embryos at 3 days post-fertilization (dpf) (developmental stage 28) correspond to early human embryos at approximately 8–15 weeks post-ovulation [12]. We demonstrated that this developmental stage (3 dpf) is the most-sensitive period during embryogenesis [13], as the highest number of apoptotic cells were identified in irradiated wild-type (wt) 3 dpf embryos, especially in the marginal area of the optic tectum (OT), which was visualized using an acridine orange (AO) assay [14-16].

Germ cells are also sensitive to irradiation, presumably because they are responsible for transmitting genetic information to next generation. If mutations occur in male germ cells, they are transmitted to offspring and can induce malformations or diseases [17, 18]. It has been demonstrated that the rates of mutation resulting from irradiation in medaka germ cells are almost equal to those of mice by nonmammalian specific-locus test system which was established by Shima *et al*. [19, 20]. The mature testes of medaka consist of many cysts containing

Preprints (www.preprints.org) | NOT PEER-REVIEWED | Posted: 1 August 2019 doi:10.20944/preprints201908.0002.v1

differentiating spermatogenic cells (spermatogonia, spermatocytes, spermatids, and spermatozoa) and spermatogonial stem cells (SSCs), each enveloped by Sertoli cells, forming a niche. Since grem cells in a cyst differentiate synchronously and all cells in the cyst are at the same stage of spermatogenesis, it is possible to identify the different spermatogenic stages by histologic examination more easily and precisely than in mammals [21-23].

The tumor suppressor protein p53, a DNA-binding transcription factor encoded by *Trp53*, plays a pivotal role as a regulator of survival and apoptosis in the developing, adult, and injured CNS [24, 25], as well as in injured gonad tissue, functioning to prevent hereditary transmission of DNA mutations affecting the reproductive system [26-29]. We examined the function of p53 with respect to regeneration in highly radiosensitive tissues, the developing CNS and matured testes, following damage induced by irradiation, by employing p53 deficient medaka which was obtained using the TILLING (Targeting Induced Local Lesions in Genomes) method [30].

Irradiation-injured neurons undergo apoptosis primarily via a p53-dependent pathway and are removed by L-plastin–expressing activated microglia

To elucidate the role of p53 in the elimination of neurons in the developing CNS that have been damaged by irradiation, we examined the temporal distribution of AO-stained apoptotic neurons in irradiated wt and p53-deficient embryos [31]. In wt 3 dpf embryonic brain irradiated

Preprints (www.preprints.org) | NOT PEER-REVIEWED | Posted: 1 August 2019 doi:10.20944/preprints201908.0002.v1

with 10 Gy of gamma rays, apoptotic cells (visualized using an AO assay) began to appear as scattered spots over the whole area of the OT at 3-5 h post-irradiation (arrows in Fig. 1A). These cells formed rosette-shaped clusters by 6 h post-irradiation, then they increased in number, enlarged, and localized in the marginal area of the OT at 10 h post-irradiation (Fig. 1B). The rosette-shaped apoptotic clusters remained obvious in the OT up to 30 h after irradiation (Fig. 1C), then disappeared completely by 42 h post-irradiation (Figs. 1D and 2). By contrast, in the irradiated brain of p53-deficient embryos, no AO-positive spots were observed at 3 h post-irradiation (Fig. 1I), but AO-positive spots were identified at 8 h post-irradiation (Fig. 2). These apoptotic neurons formed fewer, smaller clusters in the marginal area of the OT by 12 h post-irradiation (Fig. 1P) in comparison with irradiated wt embryos between 10 and 30 h post-irradiation (Fig. 1B, C, and O). Almost all of the AO-positive clusters in the OT of irradiated p53-deficient embryos disappeared within 24 h post-irradiation (Figs. 1K and 2), and AO-positive small fragments of the apoptotic neurons had disappeared completely by 42 h post-irradiation (Figs. 1L and 2). These irradiated embryos hatched and developed normally, with no evident malformations [7, 32], suggesting that the efficient elimination of apoptotic cells by phagocytosis is essential for tissue homeostasis in these multicellular organisms, consistent with previous reports [33-35].

Microglia are resident immune cells in the CNS of vertebrates that function to remove

Preprints (www.preprints.org) | NOT PEER-REVIEWED | Posted: 1 August 2019 doi:10.20944/preprints201908.0002.v1

apoptotic cells by phagocytosis following injury [36-39]. We found that the microglial marker L-plastin (lymphocyte cytosolic protein 1) was upregulated during the initial phase of the phagocytotic process, leading to a change in microglial morphology to facilitate engulfment of apoptotic neurons and increase the motility of microglia to migrate to sites of injury [31, 40]. The distribution of L-plastin–expressing microglia as determined by whole-mount *in situ* hybridization analysis of irradiated wt embryos (Fig. 1E, F, and G) was almost identical to that of AO-stained apoptotic neurons (Fig. 1A, B, and C) during 5-24 h post-irradiation. At 42 h post-irradiation, few L-plastin–expressing microglia were observed in irradiated wt embryonic brain, which was the same appearance as AO-stained apoptotic neurons (Fig. 1H). The signals of L-plastin–expressing microglia in irradiated p53-deficient embryos were smaller and fewer in number (Fig. 1M and N) compared to those of irradiated wt embryonic brain (Fig. 1E, F, and G), similar to the distribution of AO-stained apoptotic neurons in wt and p53-deficient embryos. These results strongly suggest that even in the case of deficient p53 function, irradiation-damaged cells can be removed via a p53-independent apoptotic pathway. Moreover, the AO-stained apoptotic neurons would be located in a part of the phagosome of microglia, and the phagocytic activity of microglia might not be regulated via a p53-dependent pathway.

Preprints (www.preprints.org) | NOT PEER-REVIEWED | Posted: 1 August 2019 doi:10.20944/preprints201908.0002.v1

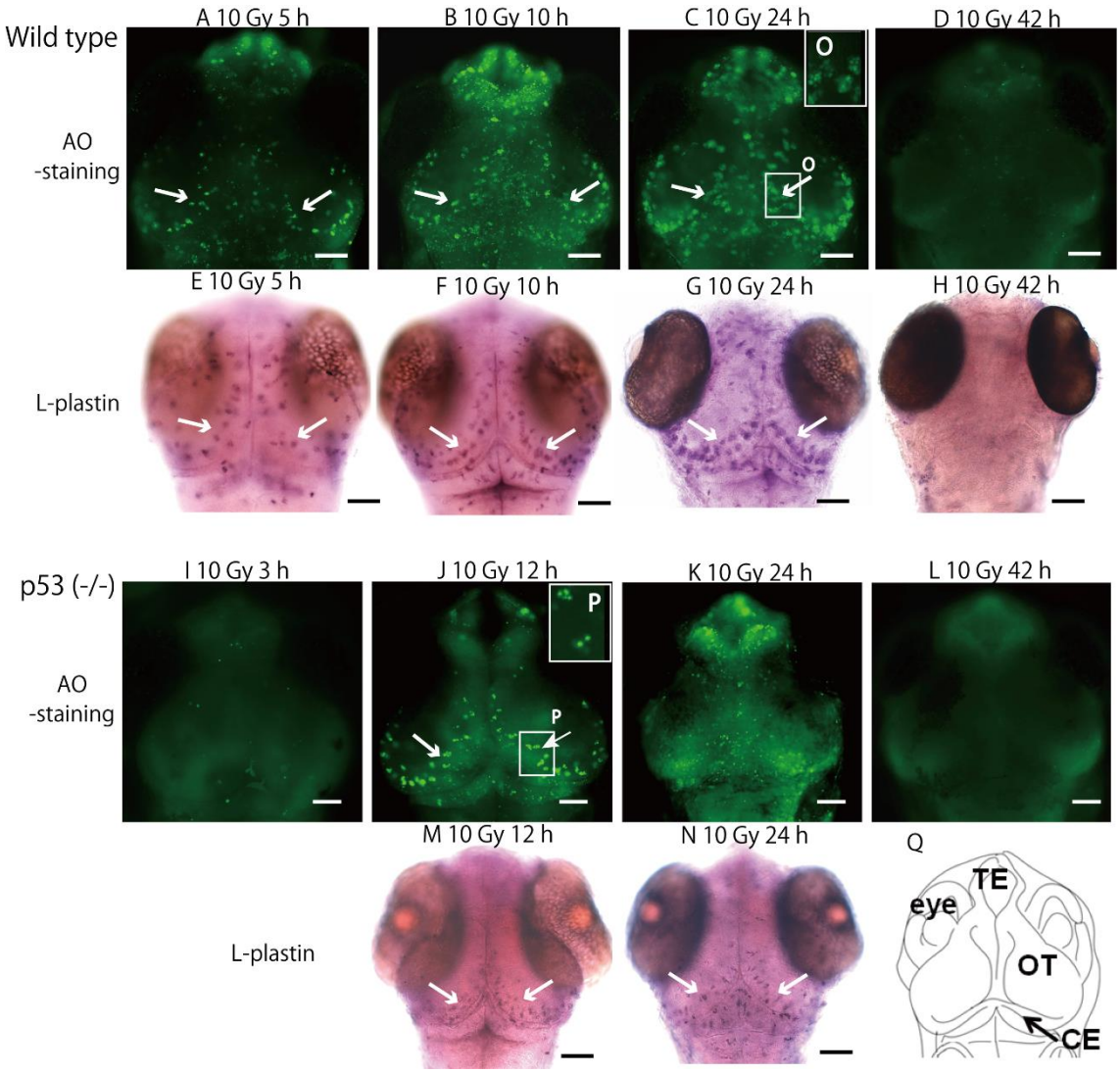

Fig. 1 Analysis of the distribution of AO-stained apoptotic neurons and activated microglia over time following irradiation of the brain in wt and p53-deficient embryos.

Embryos of wt (A-H) and p53-deficient (I-N) embryos were irradiated with 10 Gy of gamma rays and then stained with AO at 3-5 h (A, I), 10-12 h (B, J), 24 h (C, K), and 42 h (D, L) post-irradiation. AO-positive apoptotic neurons began to form rosette-shaped clusters at 5 h post-irradiation (A). The number of clustered AO-positive neurons increased, and they were located in the marginal area of the OT 10 to 24 h post-irradiation (B and C) and then disappeared by 42 h

Preprints (www.preprints.org) | NOT PEER-REVIEWED | Posted: 1 August 2019 doi:10.20944/preprints201908.0002.v1

post-irradiation (D). Images of AO-positive clusters at higher magnification for detailed views (white arrows in squares in C and J) are shown in boxes (O and P), demonstrating that clustered AO-positive neurons in the brain of p53-deficient embryos were fewer and smaller in size compared with those of wt embryos. The distribution of L-plastin expression as determined by whole-mount in situ hybridization (WISH) was identical to that of AO-positive apoptotic neurons in irradiated wt embryonic brains during 5 - 42 h post-irradiation (E-H) and in irradiated p53-deficient embryonic brains during 12 - 24 h post-irradiation (M, N). AO-stained and WISH-processed brains in A-N show dorsal views. A schematic diagram illustrating the structure of the embryonic medaka brain at stage 30 (Q). CE, cerebellum; OT, optic tectum; TE, telencephalon. Scale bars = 50 μm.

Preprints (www.preprints.org) | NOT PEER-REVIEWED | Posted: 1 August 2019 doi:10.20944/preprints201908.0002.v1

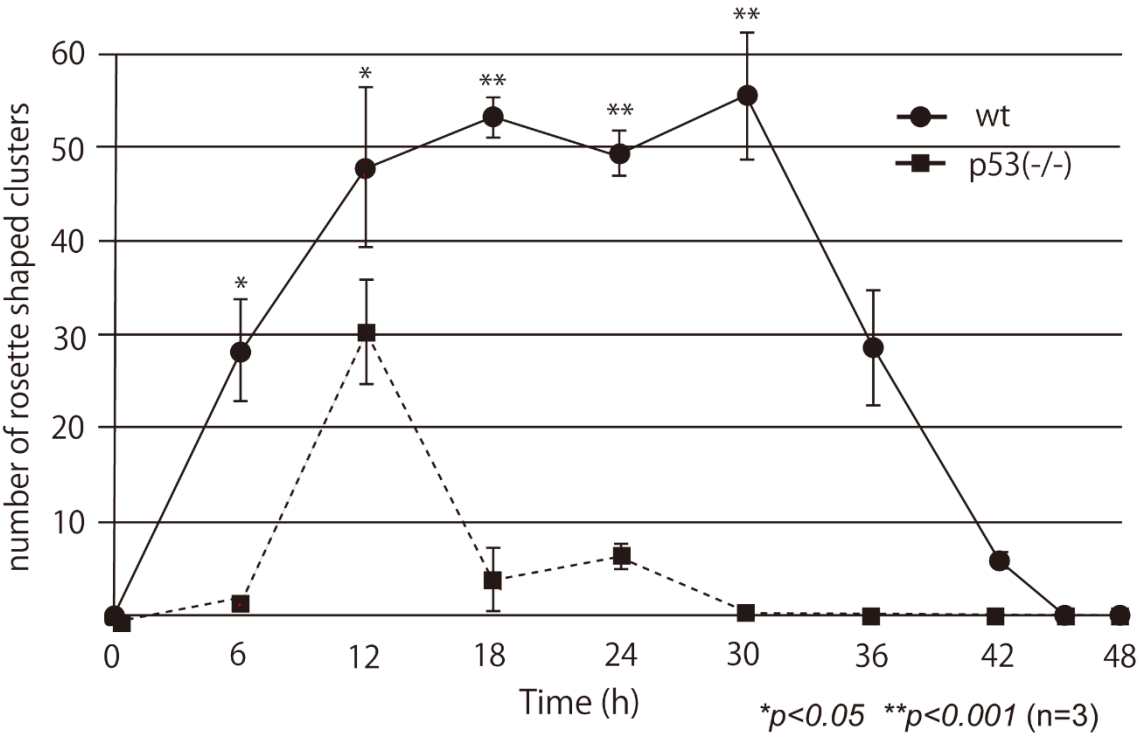

Fig. 2 Number of AO-positive rosette-shaped clusters in the OT of irradiated wt and p53-deficient embryos 48 h post-irradiation.

The number of AO-positive rosette-shaped clusters in the OT was determined at various times after gamma ray irradiation (10 Gy) of wt and p53-deficient embryos. Error bars show the SEM (n = 3). Differences between the means for wt (solid line) and p53-deficient embryos (broken line) were evaluated using Student's unpaired t tests after F tests. *P < 0.05; **P < 0.01.

Preprints (www.preprints.org) | NOT PEER-REVIEWED | Posted: 1 August 2019 doi:10.20944/preprints201908.0002.v1

Tissue regeneration in irradiation-injured embryonic brain of wt and p53-deficient embryos

In irradiated p53-deficient embryos, the clusters of AO-positive apoptotic neurons disappeared by 18 h post-irradiation, in contrast to the irradiated wt embryos, in which AO-positive apoptotic neurons remained at 36 h post-irradiation (Fig. 2). Histologic analyses using electron microscopy (EM) at 24 h post-irradiation showed that the apoptotic clusters in irradiated p53-deficient embryonic brain (arrowheads in Fig. 3B, D, and F) were much smaller and fewer in number compared with irradiated wt brain (arrowheads in Fig. 3A, C, and E). At 48 h post-irradiation in the irradiated wt embryos, condensed degenerating nuclei were observed inside round vacuoles in the retina (open arrowheads in Fig. 4D, E) and in the marginal area of the OT (arrowheads in Fig. 4D, F). Time course EM analyses of the appearance of degenerating apoptotic neurons in vacuoles confirmed that the vacuoles were a part of the phagosome of microglia involved in clearing apoptotic debris (Yasuda et al., 2015). At 48 h post-iradiation, few condensed nuclei were present in the retinal vacuoles of irradiated p53-deficient embryos (open arrowheads in Fig. 4G, H) and in the OT (arrowheads in Fig. 4G, I), presumably because the induction of apoptosis in fewer neurons (Figs. 2 and 3) would result in their being digested more quickly compared with irradiated wt embryos.

These round vacuoles were not observed in un-irradiated wt embryos at stage 34 (2 d after irradiation; 5 dpf) (Fig. 4A-C). By the time of hatching (6 d after irradiation; 9 dpf), vacuoles with

 doi:10.20944/preprints201908.0002.v1

degenerating nuclei had disappeared completely in the retina and the marginal area of the OT in both the wt and p53-deficient larvae (Fig. 4J-M); however, in irradiated wt larvae, the laminar arrangement of the retina was obviously disrupted (red bracket in Fig. 4K), and abnormal bridging structures among the layers of the retina were present (arrows in Fig. 4J, K). These abnormalities were not observed in irradiated p53-deficient larvae (Fig. 4L, M). The results of histologic analyses suggested that the irradiated wt embryos might have some defective visual capacity, although they hatched normally and developed with no apparent abnormalities in behavior upon reaching maturity [7, 32]. Our results indicating that the irradiation-injured tissues underwent self-renewal and findings of no structural abnormalities at the time of hatching in the absence of p53 suggest that p53-dependent apoptosis is not always desirable and that excessive apoptotic cell death could prevent the complete regeneration of injured tissue. Our findings suggests the possibility that the loss of p53 function could help minimize tissue damages by irradiation. Indeed, many reports have identified p53-associated neuronal loss can be one of a factor in chronic neurodegenerative conditions such as Alzheimer's disease [41-43], Parkinson's disease [44-47], Huntington's disease [48], and amyotrophic lateral sclerosis [49-51]. Another previous study by Meletis et al. [52] reported that p53 might negatively regulate self-renewal by neuronal stem cells in the adult murine brain [52]. In contrast, it was reported that p53 might play a positive role in promoting tissue self-renewal in adult medaka brain [53]. Another previous report by Otozai et

 doi:10.20944/preprints201908.0002.v1

al. demonstrated that the irradiated p53-deficient medaka exhibited markedly increased mutation frequencies by focusing on the microsatellite loci [54], which could increase the risk of carcinogenesis later in life. Future studies are thus needed to determine whether p53 plays a detrimental or beneficial role in later life in irradiated wt and p53-deficient medaka.

Preprints (www.preprints.org) | NOT PEER-REVIEWED | Posted: 1 August 2019 doi:10.20944/preprints201908.0002.v1

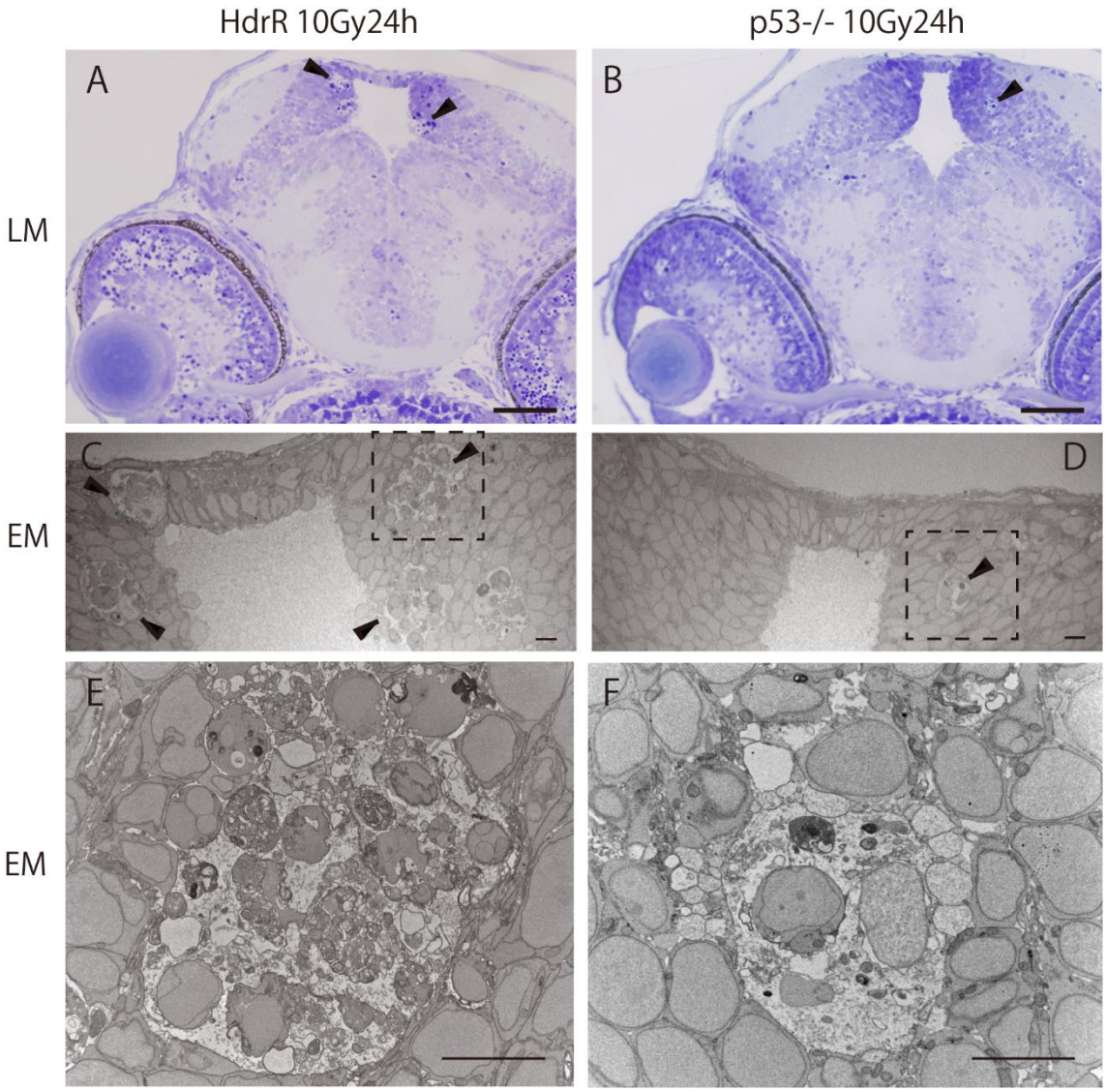

Fig. 3 Histologic features of clustered apoptotic neurons in wt and p53-deficient embryos as determined by electron microscopy (EM) at 24 h post-irradiation.

Frontal semi-thin sections stained with toluidine blue were prepared and examined by light microscopy (LM) at 24 h post-irradiation. Clustered pyknotic neurons in irradiated wt embryonic brain (arrowheads in A) and irradiated p53-deficient embryonic brain (arrowhead in B) were identified in the marginal area of the OT. EM observations demonstrated that the clustered

 doi:10.20944/preprints201908.0002.v1

apoptotic neurons in irradiated wt embryos were more numerous and larger in size (arrowheads in C and E) than those of irradiated p53-deficient embryos (arrowhead in D and F). Highly magnified views of the boxed areas in C and D correspond to E and F, respectively. Scale bars (A, B) = 50 μm; (C-F) = 5 μm.

Preprints (www.preprints.org) | NOT PEER-REVIEWED | Posted: 1 August 2019 doi:10.20944/preprints201908.0002.v1

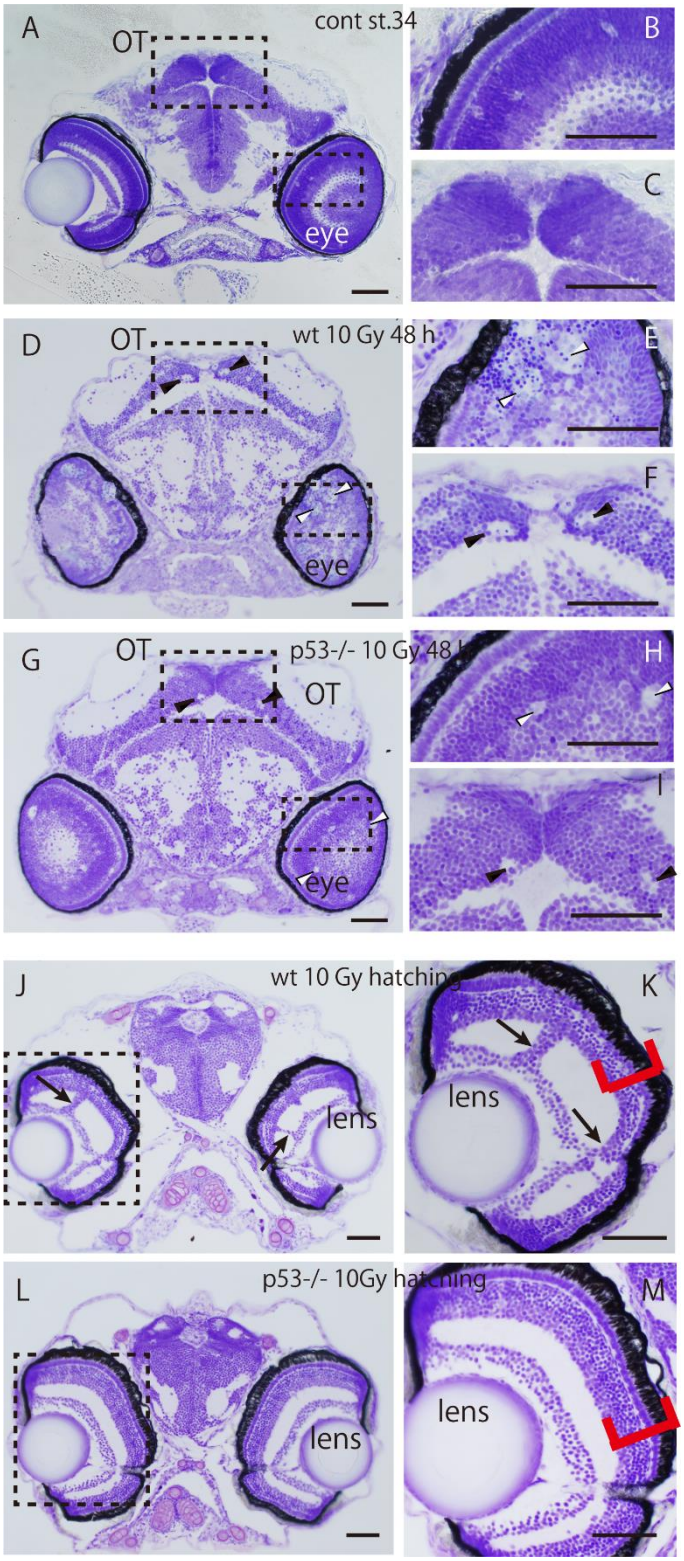

Fig. 4 Histologic analyses of irradiated embryonic brains of wt and p53-deficient embryos at 48 h post-irradiation and in the hatching period.

 doi:10.20944/preprints201908.0002.v1

Nissl-stained sections of a non-irradiated embryonic brain in developmental stage 34 showed no round vacuoles in the OT or developing retina (A). Higher magnifications of the eye and OT in the boxed areas in A are shown in B and C, respectively. At 48 h post-irradiation, wt embryos exhibited numerous round vacuoles in the OT and developing retina (D). Higher magnification of the eye and OT in the boxed areas in D shows obvious round vacuoles including condensed nuclei in the retina (open arrowheads in E) and in the marginal area of the OT (arrowheads in F) in the irradiated wt embryonic brain. In the irradiated p53-deficient embryonic brain at 48 h post-irradiation (G), similar but much smaller and fewer vacuoles were identified in the retina (open arrowheads in H) and marginal area of the OT (arrowheads in I). In the hatching period, the round vacuoles had completely disappeared in the irradiated brains of wt (J) and p53-deficient embryos (L). A higher magnification of the boxed area in J (K) shows abnormal laminar arrangements in the retina (red brackets) and abnormal structures such as bridging layers of retinal neurons (arrows) in the irradiated hatching larvae. A higher magnification of the boxed area in L shows well-ordered laminar arrangements in the retina (red brackets in M). Scale bars = 50 μm.

Preprints (www.preprints.org) | NOT PEER-REVIEWED | Posted: 1 August 2019 doi:10.20944/preprints201908.0002.v1

Radiosensitivity is dramatically altered in the brain during the later period of embryogenesis

Previous studies examining the effects of irradiation on medaka embryos demonstrated dramatic changes in viability depending on the stage at which embryos were irradiated [55, 56]. To assess the severity of biological effects following irradiation throughout the lifespan of medaka, we investigated the induction of apoptosis at 24 h post-irradiation in actively proliferating tissue, embryonic CNS at various developmental stages during late embryogenesis. We examined irradiation-induced apoptosis using light microscopy (arrows in Fig. 5B-D), an AO assay (arrows in Fig. 5F-H), and immunostaining with an anti-cleaved caspase 3 antibody (Fig. 5K-P) at 24 h post-irradiation of 3-, 4-, and 5-dpf embryos with 15 Gy of gamma rays. Light microscopic observations revealed numerous irradiation-induced opaque dead cells in the marginal area of the OT in 3 dpf embryonic brain (Fig. 5B), but the number of these cells was markedly lower in the irradiated 4 dpf embryonic brain (Fig. 5C). In contrast, no opaque dead cells were found in the irradiated 5 dpf embryonic brain (Fig. 5D). In the AO assay, the distribution of irradiation-induced apoptotic cells in the brain (Fig. 5F-H) was similar to that observed by light microscopy in irradiated 3 dpf (Fig. 5B), 4 dpf (Fig. 5C), and 5 dpf (Fig. 5D) embryos. Immunohistochemical analyses with an anti-cleaved caspase 3 antibody in irradiated 3 dpf embryos revealed extensive cleaved-caspase 3–positive apoptotic neurons in the brain and eyes (arrows in Fig. 5K and N and

 doi:10.20944/preprints201908.0002.v1

arrowheads in Fig. 5K, respectively); however, those signals were markedly lower in the brain and eyes of irradiated 4-dpf embryos (arrows in Fig. 5L and O and arrowhead in Fig. 5L, respectively). No cleaved-caspase 3–positive signals were observed in irradiated 5-dpf embryonic brain (Fig. 5M, P), similar to the results of AO staining of apoptotic neurons (Fig. 5H). These data indicate that the pattern of apoptosis following irradiation changes dramatically during the later stages of embryogenesis in medaka. Our data indicate that embryos are most sensitive to irradiation at 3 dpf, consistent with the argument of Ishikawa et al. [12] that medaka embryos at 3 dpf correspond to early human embryos at approximately 8 to 15 weeks post-ovulation, the period during which they are most sensitive to irradiation.

Preprints (www.preprints.org) | NOT PEER-REVIEWED | Posted: 1 August 2019 doi:10.20944/preprints201908.0002.v1

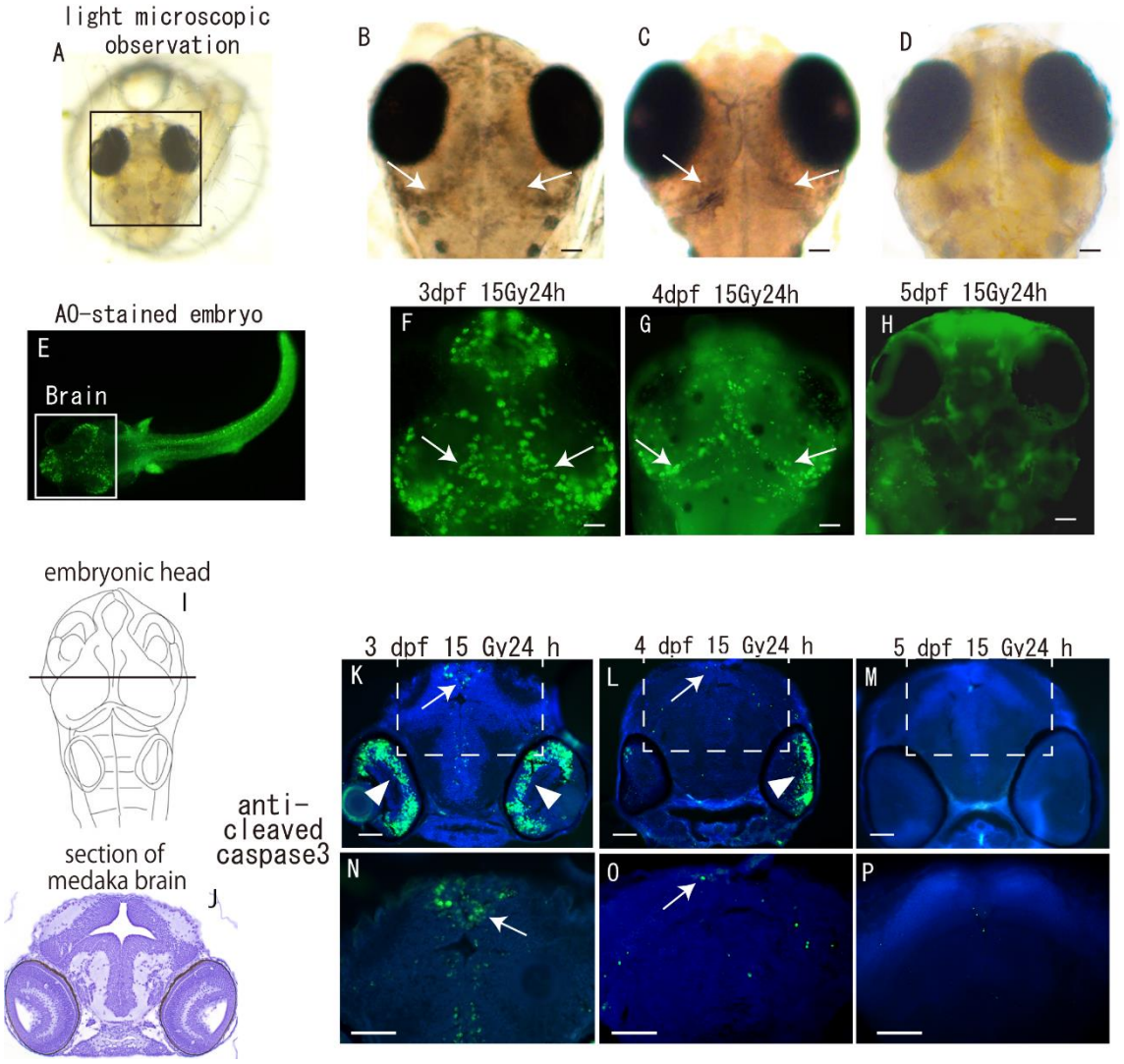

Fig. 5 The number of irradiation-induced apoptotic cells decreased markedly as embryogenesis proceeded.

Embryos at 3, 4, and 5 dpf were irradiated with 15 Gy of gamma rays, and irradiation-induced apoptotic cells in the brain (square areas in A and E) were examined by light microscopy (B-D) and AO assay (E-H) at 24 h post-irradiation. Opaque dead cells were identified in the marginal area of the OT in irradiated 3 dpf (arrows in B) and 4 dpf (arrows in C) embryonic brains. In irradiated 5 dpf embryonic brains, no opaque dead cells were evident (D). The distribution of AO-

 doi:10.20944/preprints201908.0002.v1

stained apoptotic cells in the brain of irradiated 3 - 5 dpf embryos (arrows in F, G) was similar to that in the microscopic observations (arrows in B, C). Panels I and J show schematic illustrations of the embryonic head and sections of the embryonic brain. Frontal cryo-sections of the embryonic brain were prepared at the level of the solid line shown in I (K-P). Immunohistochemical sections stained with anti-cleaved caspase 3 antibody at 24 h post-irradiation of 3 dpf (K), 4 dpf (L), and 5 dpf (M) embryos were prepared. Magnified images in square areas with dotted outlines in K, L, and M are shown in N, O, and P, respectively. In irradiated 3 dpf embryos, cleaved-caspase 3–positive apoptotic neurons were present in the brain (arrows in K, N) and eyes (arrowheads in K). Fewer apoptotic cells were found in the brain (arrows in L, O) and eyes (arrowhead in L) of irradiated 4-dpf embryos, and no signals were detected in irradiated 5-dpf embryos (M, P). Scale bars = 50 μm.

Preprints (www.preprints.org) | NOT PEER-REVIEWED | Posted: 1 August 2019 doi:10.20944/preprints201908.0002.v1

Irradiation promotes mis-differentiation during spermatogenesis in p53-deficient medaka testes

Previous studies by Kuwahara et al. suggested that irradiation-induced genomic lesions in germ cells are eliminated in one of two ways: either by DNA repair and apoptosis, or by a reset system of spermatogenesis. Surviving irradiated spermatogenic cells, except for SSCs, are prematurely removed from the testis by acceleration of spermatogenesis [57, 58]. To fully characterize the role of p53 in irradiation-disrupted spermatogenesis, we examined the histologic changes in irradiated testes of wt and p53-deficient medaka. In wt testis at 1 d post-irradiation with 5 Gy of gamma-rays, strongly HE-stained pyknotic cells (arrows in Fig. 6A) that were positive for anti-cleaved caspase 3 (arrows in Fig. 6B) were observed in the cysts of early differentiating spermatogonia. Almost all apoptotic cells disappeared within 7 d post-irradiation (Fig. 6C, D). At 7 d post-irradiation, the number of cysts of early differentiating spermatogonia and spermatocytes decreased markedly, and the majority of the area of the irradiated testis tissue was occupied by cysts with spermatids and sperm (Fig. 6C). In addition, the somatic cells that formed the boundaries of the cysts were hypertrophied, as shown in the red solid area in Figure 6D, which were consistent with the findings reported by Kuwahara et al [57, 58]. This same histologic appearance was observed at 14 d post-irradiation (Fig. 6E); however, spermatogenesis was completely restored by 28 d post-irradiation (Fig. 6F, G).

Preprints (www.preprints.org) | NOT PEER-REVIEWED | Posted: 1 August 2019 doi:10.20944/preprints201908.0002.v1

In the testes of irradiated p53-deficient medaka, no pyknotic cells were observed up to 3 d post-irradiation. At that time, we observed small ovum-like cells (testis-ova) in the cysts of SSCs (arrowheads in Fig. 6I). The number of testis-ova cells had increased markedly and they had become larger in size in the cysts of SSCs and early differentiating spermatogonia by 14 d post-irradiation (arrowheads in Fig. 6J). However, almost all of the testis-ova disappeared in the irradiated p53-deficient testes by 28 d post-irradiation (Fig. 6K, L), demonstrating the restoration of spermatogenesis, similar to irradiated wt testes. Although the medaka have an XX/XY sex chromosome system [59-61], environmental factors such as high temperature [62, 63], starvation [64] can induce female-to-male sex reversal in the recovering process of spermatogenesis. This suggests that medaka germ cells exhibit sexual bipotentiality. Furthermore, in testes of adult medaka, testis-ova cells can be produced following impairment by administration of sex steroids [65-69]. We found no apoptotic cells in irradiated p53-deficient testes at 3 d post-irradiation, in contrast to irradiated wt testes, in which many pyknotic cells appeared at 1 d post-irradiation. Instead, at 3 d post-irradiation, trans-differentiation of SSCs into oocyte-like cells, known as testis-ova cells, was observed in irradiated p53-deficient testes. This finding strongly suggests that irradiation disrupts the normal differentiation of spermatogonia, inducing mis-differentiation of spermatogonia into ovum-like cells in the absence of p53 activity. In wt testes, mis-differentiated testis-ova would be removed via p53-

 doi:10.20944/preprints201908.0002.v1

dependent apoptosis, whereas in p53-deficient testes, mis-differentiated testis-ova might survive and grow, presumably because their removal was disrupted by the delay in the induction of apoptosis. Thereafter, p53-independent apoptosis might eliminate almost all abnormally generated testis-ova cells within 28 d after irradiation. Our results strongly suggest that spermatogenesis is completely restored by p53-independent apoptosis, even in the case of p53 functional deficiency.

Preprints (www.preprints.org) | NOT PEER-REVIEWED | Posted: 1 August 2019 doi:10.20944/preprints201908.0002.v1

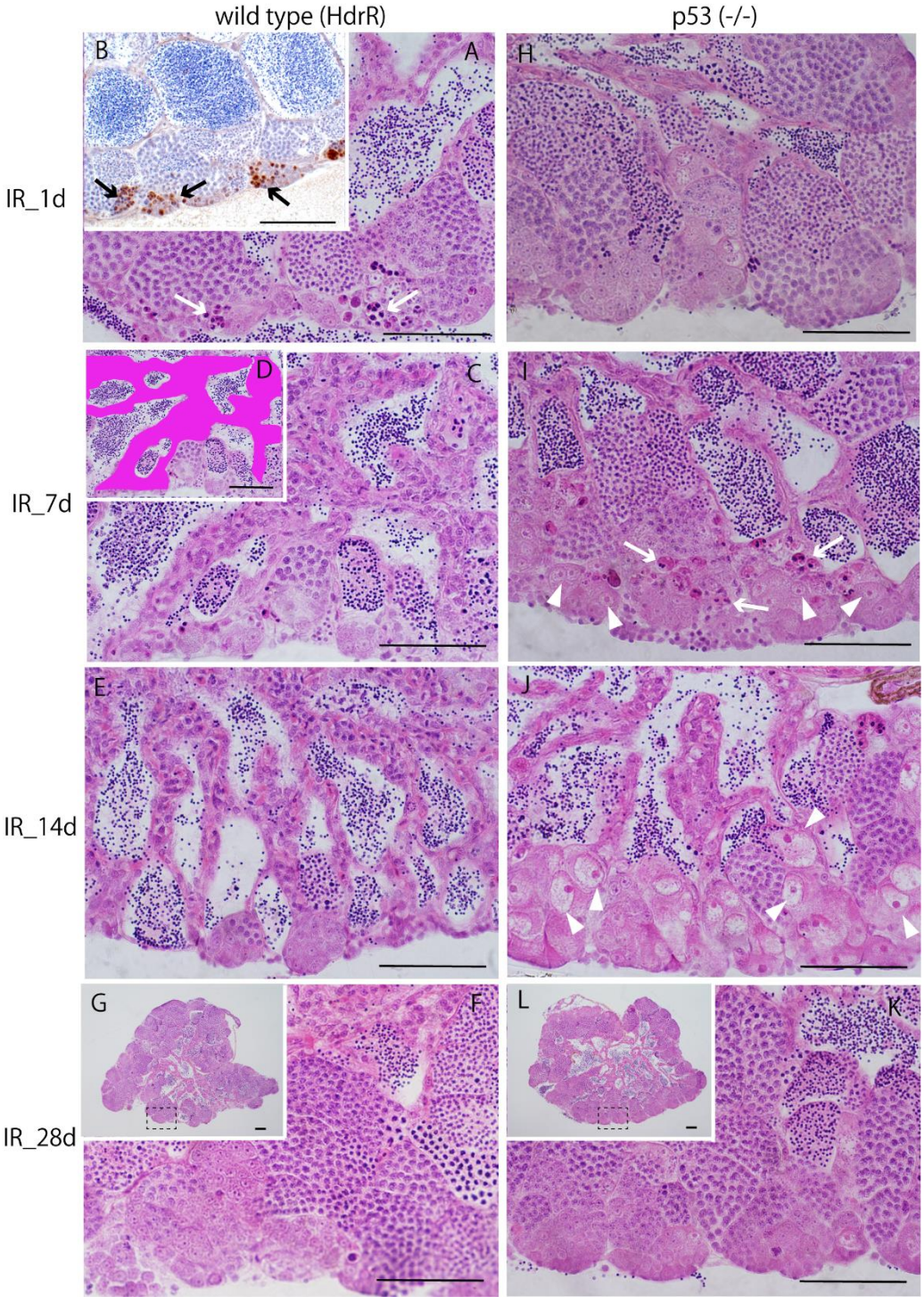

Fig. 6 Histologic changes in irradiated wt and p53-deficient testes over a period of 28 d (1 month) following irradiation with 5 Gy of gamma-rays

Hematoxylin-eosin (HE)-stained sections of wt testes showed numerous pyknotic cells in the

 doi:10.20944/preprints201908.0002.v1

cysts of early differentiating spermatogonia (arrows in A). Histologic analyses of sections immune-stained with anti-cleaved caspase 3 antibody indicated the presence of immune-positive apoptotic neurons in the cysts (arrows in B) where pyknotic cells (arrows in A) were present. Histologic analyses of HE-stained sections of wt testes at 7 d post-irradiation revealed the appearance of hypertrophied Sertoli cells (C). A schematic representation of the hypertrophied Sertoli cells (red) in (C) is shown in (D). Histologic analyses of HE-stained sections showed that the characteristic appearance of hypertrophied Sertoli cells continued through 14 d post-irradiation (E). Histologic analyses of HE-stained sections of wt testes 28 d post-irradiation (G) and an enlarged view of the boxed area in (G) clearly demonstrate the restoration of spermatogenesis (F). No apparent histologic changes were noted in HE-stained sections in irradiated p53-deficient medaka at 1 d post-irradiation (H). At 7 d post-irradiation, many pyknotic cells were present (arrows in I), and numerous ovum-like cells (testis-ova) were present in the cysts of SSC and early differentiating spermatogonia (arrowheads in I). The number of testis-ova increased markedly, and they had increased in size in the cysts of SSC and early differentiating spermatogonia by 14 d post-irradiation (arrowheads in J). However, almost all testis-ova cells had disappeared by 28 d post-irradiation (L). A magnified image of the squared area in L clearly demonstrates the restoration of spermatogenesis (K). Scale bars = 50 µm.

Preprints (www.preprints.org) | NOT PEER-REVIEWED | Posted: 1 August 2019 doi:10.20944/preprints201908.0002.v1

Conclusion

We found that p53-independent apoptosis plays a role in the efficient elimination of irradiation-induced apoptotic neurons in the developing CNS of p53-deficient medaka and in the removal of abnormally differentiated testis-ova generated by irradiation of mature testes. Collectively, our data suggest that even if the function of p53 (which normally regulates the induction of apoptosis) is deficient, removal of irradiation-generated damaged cells and restoration of injured tissues occurs via a p53-independent apoptosis pathway. Our findings suggest that p53 is not indispensable for tissue restoration; however, it might be associated with increased risk of carcinogenesis later in life due to the probability of survival of neurons with severely damaged DNA in the CNS and increased frequency of mis-differentiation in gonadal tissue following irradiation.

Preprints (www.preprints.org) | NOT PEER-REVIEWED | Posted: 1 August 2019 doi:10.20944/preprints201908.0002.v1

Figure legends

Fig. 1 Analysis of the distribution of AO-stained apoptotic neurons and activated microglia over time following irradiation of the brain in wt and p53-deficient embryos.

Embryos of wt (A-H) and p53-deficient (I-N) embryos were irradiated with 10 Gy of gamma rays and then stained with AO at 3-5 h (A, I), 10-12 h (B, J), 24 h (C, K), and 42 h (D, L) post-irradiation. AO-positive apoptotic neurons began to form rosette-shaped clusters at 5 h post-irradiation (A). The number of clustered AO-positive neurons increased, and they were located in the marginal area of the OT 10 to 24 h post-irradiation (B and C) and then disappeared by 42 h post-irradiation (D). Images of AO-positive clusters at higher magnification for detailed views (white arrows in squares in C and J) are shown in boxes (O and P), demonstrating that clustered AO-positive neurons in the brain of p53-deficient embryos were fewer and smaller in size compared with those of wt embryos. The distribution of L-plastin expression as determined by whole-mount in situ hybridization (WISH) was identical to that of AO-positive apoptotic neurons in irradiated wt embryonic brains during 5 - 42 h post-irradiation (E-H) and in irradiated p53-deficient embryonic brains during 12 - 24 h post-irradiation (M, N). AO-stained and WISH-processed brains in A-N show dorsal views. A schematic diagram illustrating the structure of the embryonic medaka brain at stage 30 (Q). CE, cerebellum; OT, optic tectum; TE, telencephalon.

Preprints (www.preprints.org) | NOT PEER-REVIEWED | Posted: 1 August 2019 doi:10.20944/preprints201908.0002.v1

Scale bars = 50 μm.

Fig. 2 Number of AO-positive rosette-shaped clusters in the OT of irradiated wt and p53-deficient embryos 48 h post-irradiation.

The number of AO-positive rosette-shaped clusters in the OT was determined at various times after gamma ray irradiation (10 Gy) of wt and p53-deficient embryos. Error bars show the SEM (n = 3). Differences between the means for wt (solid line) and p53-deficient embryos (broken line) were evaluated using Student's unpaired t tests after F tests. *$P < 0.05$; **$P < 0.01$.

Fig. 3 Histologic features of clustered apoptotic neurons in wt and p53-deficient embryos as determined by electron microscopy (EM) at 24 h post-irradiation.

Frontal semi-thin sections stained with toluidine blue were prepared and examined by light microscopy (LM) at 24 h post-irradiation. Clustered pyknotic neurons in irradiated wt embryonic brain (arrowheads in A) and irradiated p53-deficient embryonic brain (arrowhead in B) were identified in the marginal area of the OT. EM observations demonstrated that the clustered apoptotic neurons in irradiated wt embryos were more numerous and larger in size (arrowheads in C and E) than those of irradiated p53-deficient embryos (arrowhead in D and F). Highly magnified views of the boxed areas in C and D correspond to E and F, respectively. Scale bars (A,

Preprints (www.preprints.org) | NOT PEER-REVIEWED | Posted: 1 August 2019 doi:10.20944/preprints201908.0002.v1

B) = 50 μm; (C-F) = 5 μm.

Fig. 4 Histologic analyses of irradiated embryonic brains of wt and p53-deficient embryos at 48 h post-irradiation and in the hatching period

Nissl-stained sections of a non-irradiated embryonic brain in developmental stage 34 showed no round vacuoles in the OT or developing retina (A). Higher magnifications of the eye and OT in the boxed areas in A are shown in B and C, respectively. At 48 h post-irradiation, wt embryos exhibited numerous round vacuoles in the OT and developing retina (D). Higher magnification of the eye and OT in the boxed areas in D shows obvious round vacuoles including condensed nuclei in the retina (open arrowheads in E) and in the marginal area of the OT (arrowheads in F) in the irradiated wt embryonic brain. In the irradiated p53-deficient embryonic brain at 48 h post-irradiation (G), similar but much smaller and fewer vacuoles were identified in the retina (open arrowheads in H) and marginal area of the OT (arrowheads in I). In the hatching period, the round vacuoles had completely disappeared in the irradiated brains of wt (J) and p53-deficient embryos (L). A higher magnification of the boxed area in J (K) shows abnormal laminar arrangements in the retina (red brackets) and abnormal structures such as bridging layers of retinal neurons (arrows) in the irradiated hatching larvae. A higher magnification of the boxed area in L shows well-ordered laminar arrangements in the retina (red brackets in M). Scale bars = 50 μm.

 doi:10.20944/preprints201908.0002.v1

Fig. 5 The number of irradiation-induced apoptotic cells decreased markedly as embryogenesis proceeded.

Embryos at 3, 4, and 5 dpf were irradiated with 15 Gy of gamma rays, and irradiation-induced apoptotic cells in the brain (square areas in A and E) were examined by light microscopy (B-D) and AO assay (E-H) at 24 h post-irradiation. Opaque dead cells were identified in the marginal area of the OT in irradiated 3 dpf (arrows in B) and 4 dpf (arrows in C) embryonic brains. In irradiated 5 dpf embryonic brains, no opaque dead cells were evident (D). The distribution of AO-stained apoptotic cells in the brain of irradiated 3 - 5 dpf embryos (arrows in F, G) was similar to that in the microscopic observations (arrows in B, C). Panels I and J show schematic illustrations of the embryonic head and sections of the embryonic brain. Frontal cryo-sections of the embryonic brain were prepared at the level of the solid line shown in I (K-P). Immunohistochemical sections stained with anti-cleaved caspase 3 antibody at 24 h post-irradiation of 3 dpf (K), 4 dpf (L), and 5 dpf (M) embryos were prepared. Magnified images in square areas with dotted outlines in K, L, and M are shown in N, O, and P, respectively. In irradiated 3 dpf embryos, cleaved-caspase 3–positive apoptotic neurons were present in the brain (arrows in K, N) and eyes (arrowheads in K). Fewer apoptotic cells were found in the brain (arrows in L, O) and eyes (arrowhead in L) of irradiated 4-dpf embryos, and no signals were

Preprints (www.preprints.org) | NOT PEER-REVIEWED | Posted: 1 August 2019 doi:10.20944/preprints201908.0002.v1

detected in irradiated 5-dpf embryos (M, P). Scale bars = 50 μm.

Fig. 6 Histologic changes in irradiated wt and p53-deficient testes over a period of 28 d (1 month) following irradiation with 5 Gy of gamma-rays

Hematoxylin-eosin (HE)-stained sections of wt testes showed numerous pyknotic cells in the cysts of early differentiating spermatogonia (arrows in A). Histologic analyses of sections immune-stained with anti-cleaved caspase 3 antibody indicated the presence of immune-positive apoptotic neurons in the cysts (arrows in B) where pyknotic cells (arrows in A) were present. Histologic analyses of HE-stained sections of wt testes at 7 d post-irradiation revealed the appearance of hypertrophied Sertoli cells (C). A schematic representation of the hypertrophied Sertoli cells (red) in (C) is shown in (D). Histologic analyses of HE-stained sections showed that the characteristic appearance of hypertrophied Sertoli cells continued through 14 d post-irradiation (E). Histologic analyses of HE-stained sections of wt testes 28 d post-irradiation (G) and an enlarged view of the boxed area in (G) clearly demonstrate the restoration of spermatogenesis (F). No apparent histologic changes were noted in HE-stained sections in irradiated p53-deficient medaka at 1 d post-irradiation (H). At 7 d post-irradiation, many pyknotic cells were present (arrows in I), and numerous ovum-like cells (testis-ova) were present in the cysts of SSC and early differentiating spermatogonia (arrowheads in I). The number of testis-ova

 doi:10.20944/preprints201908.0002.v1

increased markedly, and they had increased in size in the cysts of SSC and early differentiating spermatogonia by 14 d post-irradiation (arrowheads in J). However, almost all testis-ova cells had disappeared by 28 d post-irradiation (L). A magnified image of the squared area in L clearly demonstrates the restoration of spermatogenesis (K). Scale bars = 50 μm.

 doi:10.20944/preprints201908.0002.v1

Acknowledgements

This work was supported by Grants-in-Aid for Scientific Research from the Ministry of Education, Culture, Sports, Science and Technology (MEXT) of Japan (16K00541, 22510056 and 25514002 to TY), and the Gold Ribbon Network, Approved Specified Non-profit Corporation to TY.

Conflicts of Interest: The authors declare no conflict of interest.

 doi:10.20944/preprints201908.0002.v1

References

1. Yamamoto, T., *Medaka (killifish) : biology and strains*. Yugaku-sha : distributed by Keigaku Pub. Co.: Tokyo, 1975; p 365 p., 18 leaves of plates.

2. Egami, N.; Yamagami, K.; Shima, A., *Medaka no seibutsugaku*. Shohan. ed.; Tōkyō Daigaku Shuppankai: Tōkyō, 1990; p v, 315 p.

3. Iwamatsu, T., The Biology of the Medaka. **1993**.

4. Naruse, K.; Sakaizumi, M.; Shima, A., Medaka as a model organism for research in experimental biology. *The Fish Biology Journal Medaka* **1994,** 6, 47-52.

5. Ishikawa, Y.; HyodoTaguchi, Y.; Tatsumi, K., Medaka fish for mutant screens. *Nature* **1997,** 386, (6622), 234-234.

6. Shima, A.; Mitani, H., Medaka as a research organism: past, present and future. *Mechanisms of development* **2004,** 121, (7-8), 599-604.

7. Yasuda, T.; Aoki, K.; Matsumoto, A.; Maruyama, K.; Hyodo-Taguchi, Y.; Fushiki, S.; Ishikawa, Y., Radiation-induced brain cell death can be observed in living Medaka embryos. *Journal of radiation research* **2006,** 47, (3-4), 295-303.

8. Murata, Y.; Yasuda, T.; Watanabe-Asaka, T.; Oda, S.; Mantoku, A.; Takeyama, K.; Chatani, M.; Kudo, A.; Uchida, S.; Suzuki, H.; Tanigaki, F.; Shirakawa, M.; Fujisawa,

 doi:10.20944/preprints201908.0002.v1

K.; Hamamoto, Y.; Terai, S.; Mitani, H., Histological and Transcriptomic Analysis of Adult Japanese Medaka Sampled Onboard the International Space Station. *PloS one* **2015,** 10, (10).

9. Nagata, K.; Hashimoto, C.; Watanabe-Asaka, T.; Itoh, K.; Yasuda, T.; Ohta, K.; Oonishi, H.; Igarashi, K.; Suzuki, M.; Funayama, T.; Kobayashi, Y.; Nishimaki, T.; Katsumura, T.; Oota, H.; Ogawa, M.; Oga, A.; Ikemoto, K.; Itoh, H.; Kutsuna, N.; Oda, S.; Mitani, H., In vivo 3D analysis of systemic effects after local heavy-ion beam irradiation in an animal model. *Scientific reports* **2016,** 6, 28691.

10. Ishikawa, Y., Medakafish as a model system for vertebrate developmental genetics. *Bioessays* **2000,** 22, (5), 487-495.

11. Furutani-Seiki, M.; Wittbrodt, J., Medaka and zebrafish, an evolutionary twin study. *Mechanisms of development* **2004,** 121, (7-8), 629-637.

12. Ishikawa, Y.; Yasuda, T.; Kage, T.; Takashima, S.; Yoshimoto, M.; Yamamoto, N.; Maruyama, K.; Takeda, H.; Ito, H., Early development of the cerebellum in teleost fishes: A study based on gene expression patterns and histology in the medaka embryo. *Zool Sci* **2008,** 25, (4), 407-418.

13. Yasuda, T.; Ishikawa, Y.; Shioya, N.; Itoh, K.; Kamahori, M.; Nagata, K.; Takano, Y.; Mitani, H.; Oda, S., Radical change of apoptotic strategy following irradiation during

later period of embryogenesis in medaka (Oryzias latipes). *PloS one* **2018,** 13, (8), e0201790.

14. Yasuda, T.; Yoshimoto, M.; Maeda, K.; Matsumoto, A.; Maruyama, K.; Ishikawa, Y., Rapid and Simple Method for Quantitative Evaluation of Neurocytotoxic Effects of Radiation on Developing Medaka Brain. *Journal of radiation research* **2008,** 49, (5), 533-540.

15. Yasuda, T.; Oda, S.; Ishikawa, Y.; Watanabe-Asaka, T.; Hidaka, M.; Yasuda, H.; Anzai, K.; Mitani, H., Live imaging of radiation-induced apoptosis by yolk injection of Acridine Orange in the developing optic tectum of medaka. *Journal of radiation research* **2009,** 50, (6), 487-94.

16. Yasuda, T.; Oda, S.; Yasuda, H.; Hibi, Y.; Anzai, K.; Mitani, H., Neurocytotoxic effects of iron-ions on the developing brain measured in vivo using medaka (Oryzias latipes), a vertebrate model. *Int J Radiat Biol* **2011,** 87, (9), 915-922.

17. Russell, W. L.; Russell, L. B.; Kelly, E. M., Radiation dose rate and mutation frequency. *Science (New York, N.Y.)* **1958,** 128, (3338), 1546-50.

18. Russell, W. L.; Kelly, E. M., Mutation frequencies in male mice and the estimation of genetic hazards of radiation in men. *Proceedings of the National Academy of Sciences of the United States of America* **1982,** 79, (2), 542-4.

 doi:10.20944/preprints201908.0002.v1

19. Shima, A.; Shimada, A., Induction of Mutations in Males of the Fish Oryzias-Latipes at a Specific Locus after Gamma-Irradiation. *Mutation research* **1988,** 198, (1), 93-98.

20. Shima, A.; Shimada, A., Development of a Possible Nonmammalian Test System for Radiation-Induced Germ-Cell Mutagenesis Using a Fish, the Japanese Medaka (Oryzias-Latipes). *Proceedings of the National Academy of Sciences of the United States of America* **1991,** 88, (6), 2545-2549.

21. Grier, H. J.; Horner, J.; Mahesh, V. B., The Morphology of Enclosed Testicular Tubules in a Teleost Fish, Poecilia-Latipinna. *T Am Microsc Soc* **1980,** 99, (3), 268-276.

22. Grier, H. J.; Linton, J. R.; Leatherland, J. F.; De Vlaming, V. L., Structural evidence for two different testicular types in teleost fishes. *The American journal of anatomy* **1980,** 159, (3), 331-45.

23. Kanamori, A.; Nagahama, Y.; Egami, N., Development of the Tissue Architecture in the Gonads of the Medaka Oryzias-Latipes. *Zool Sci* **1985,** 2, (5), 695-706.

24. Jacobs, W. B.; Kaplan, D. R.; Miller, F. D., The p53 family in nervous system development and disease. *J Neurochem* **2006,** 97, (6), 1571-1584.

25. Borges, H. L.; Linden, R.; Wang, J. Y. J., DNA damage-induced cell death: lessons from the central nervous system. *Cell research* **2008,** 18, (1), 17-26.

26. Xu, G. G.; Vogel, K. S.; McMahan, C. A.; Herbert, D. C.; Walter, C. A., BAX and Tumor

Suppressor TRP53 Are Important in Regulating Mutagenesis in Spermatogenic Cells in Mice. *Biology of reproduction* **2010,** 83, (6), 979-987.

27. Le, W.; Qi, L. X.; Li, J. X.; Wu, D. L.; Xu, J.; Zhang, J. F., Low-dose ionizing irradiation triggers a 53BP1 response to DNA double strand breaks in mouse spermatogonial stem cells. *Syst Biol Reprod Med* **2016,** 62, (2), 106-113.

28. Banerjee, S.; Chaturvedi, C. M., Apoptotic mechanism behind the testicular atrophy in photorefractory and scotosensitive quail: Involvement of GnIH induced p-53 dependent Bax-Caspase-3 mediated pathway. *J Photoch Photobio B* **2017,** 176, 124-135.

29. Zamir-Nasta, T.; Razi, M.; Shapour, H.; Malekinejad, H., Roles of p21, p53, cyclin D1, CDK-4, estrogen receptor in aflatoxin B1-induced cytotoxicity in testicular tissue of mice. *Environ Toxicol* **2018,** 33, (4), 385-395.

30. Taniguchi, Y.; Takeda, S.; Furutani-Seiki, M.; Kamei, Y.; Todo, T.; Sasado, T.; Deguchi, T.; Kondoh, H.; Mudde, J.; Yamazoe, M.; Hidaka, M.; Mitani, H.; Toyoda, A.; Sakaki, Y.; Plasterk, R. H.; Cuppen, E., Generation of medaka gene knockout models by target-selected mutagenesis. *Genome biology* **2006,** 7, (12), R116.

31. Yasuda, T.; Oda, S.; Hibi, Y.; Satoh, S.; Nagata, K.; Hirakawa, K.; Kutsuna, N.; Sagara, H.; Mitani, H., Embryonic Medaka Model of Microglia in the Developing CNS Allowing In Vivo Analysis of Their Spatiotemporal Recruitment in Response to Irradiation. *PloS*

one **2015,** 10, (6), e0127325.

32. Yasuda, T.; Kimori, Y.; Nagata, K.; Igarashi, K.; Watanabe-Asaka, T.; Oda, S.; Mitani, H., Irradiation-injured brain tissues can self-renew in the absence of the pivotal tumor suppressor p53 in the medaka (Oryzias latipes) embryo. *Journal of radiation research* **2016,** 57, (1), 9-15.

33. Lauber, K.; Blumenthal, S. G.; Waibel, M.; Wesselborg, S., Clearance of apoptotic cells: Getting rid of the corpses. *Molecular cell* **2004,** 14, (3), 277-287.

34. Platt, N.; da Silva, R. P.; Gordon, S., Class A scavenger receptors and the phagocytosis of apoptotic cells. *Biochemical Society transactions* **1998,** 26, (4), 639-644.

35. Platt, N.; da Silva, R. P.; Gordon, S., Recognizing death: the phagocytosis of apoptotic cells. *Trends Cell Biol* **1998,** 8, (9), 365-372.

36. Ransohoff, R. M.; Cardona, A. E., The myeloid cells of the central nervous system parenchyma. *Nature* **2010,** 468, (7321), 253-262.

37. Eyo, U.; Dailey, M. E., Effects of oxygen-glucose deprivation on microglial mobility and viability in developing mouse hippocampal tissues. *Glia* **2012,** 60, (11), 1747-1760.

38. Prinz, M.; Priller, J., Microglia and brain macrophages in the molecular age: from origin to neuropsychiatric disease. *Nature Reviews Neuroscience* **2014,** 15, (5), 300-312.

39. Lyons, D. A.; Talbot, W. S., Glial Cell Development and Function in Zebrafish. *Csh*

Perspect Biol **2015,** 7, (2).

40. Yasuda, T.; Kamahori, M.; Nagata, K.; Watanabe-Asaka, T.; Suzuki, M.; Funayama, T.; Mitani, H.; Oda, S., Abscopal Activation of Microglia in Embryonic Fish Brain Following Targeted Irradiation with Heavy-Ion Microbeam. *International journal of molecular sciences* **2017,** 18, (7).

41. Anderson, A. J.; Stoltzner, S.; Lai, F.; Su, J.; Nixon, R. A., Morphological and biochemical assessment of DNA damage and apoptosis in Down syndrome and Alzheimer disease, and effect of postmortem tissue archival on TUNEL. *Neurobiol Aging* **2000,** 21, (4), 511-524.

42. Sajan, F. D.; Martiniuk, F.; Marcus, D. L.; Frey, W. H., 2nd; Hite, R.; Bordayo, E. Z.; Freedman, M. L., Apoptotic gene expression in Alzheimer's disease hippocampal tissue. *American journal of Alzheimer's disease and other dementias* **2007,** 22, (4), 319-28.

43. Su, J. H.; Satou, T.; Anderson, A. J.; Cotman, C. W., Up-regulation of Bcl-2 is associated with neuronal DNA damage in Alzheimer's disease. *Neuroreport* **1996,** 7, (2), 437-440.

44. Burguillos, M. A.; Deierborg, T.; Kavanagh, E.; Persson, A.; Hajji, N.; Garcia-Quintanilla, A.; Cano, J.; Brundin, P.; Englund, E.; Venero, J. L.; Joseph, B., Caspase signalling controls microglia activation and neurotoxicity. *Nature* **2011,** 472, (7343), 319-U214.

45. Tatton, N. A., Increased caspase 3 and Bax immunoreactivity accompany nuclear

GAPDH translocation and neuronal apoptosis in Parkinson's disease. *Exp Neurol* **2000,** 166, (1), 29-43.

46. Gandhi, S.; Wood, N. W., Molecular pathogenesis of Parkinson's disease. *Hum Mol Genet* **2005,** 14, 2749-2755.

47. Schapira, A. H.; Jenner, P., Etiology and Pathogenesis of Parkinson's Disease. *Movement Disord* **2011,** 26, (6), 1049-1055.

48. Illuzzi, J. L.; Vickers, C. A.; Kmiec, E. B., Modifications of p53 and the DNA Damage Response in Cells Expressing Mutant Form of the Protein Huntingtin. *J Mol Neurosci* **2011,** 45, (2), 256-268.

49. Martin, L. J., p53 is abnormally elevated and active in the CNS of patients with amyotrophic lateral sclerosis. *Neurobiol Dis* **2000,** 7, (6), 613-622.

50. Ranganathan, S.; Bowser, R., p53 and Cell Cycle Proteins Participate in Spinal Motor Neuron Cell Death in ALS. *The open pathology journal* **2010,** 4, 11-22.

51. Eve, D. J.; Dennis, J. S.; Citron, B. A., Transcription factor p53 in degenerating spinal cords. *Brain Res* **2007,** 1150, 174-181.

52. Meletis, K.; Wirta, V.; Hede, S. M.; Nister, M.; Lundeberg, J.; Frisen, J., P53 suppresses the self-renewal of adult neural stem cells. *Development* **2006,** 133, (2), 363-369.

53. Isoe, Y.; Okuyama, T.; Taniguchi, Y.; Kubo, T.; Takeuchi, H., p53 Mutation suppresses

 doi:10.20944/preprints201908.0002.v1

adult neurogenesis in medaka fish (Oryzias latipes). *Biochem Bioph Res Co* **2012,** 423, (4), 627-631.

54. Otozai, S.; Ishikawa-Fujiwara, T.; Oda, S.; Kamei, Y.; Ryo, H.; Sato, A.; Nomura, T.; Mitani, H.; Tsujimura, T.; Inohara, H.; Todo, T., p53-Dependent suppression of genome instability in germ cells. *Mutat Res-Fund Mol M* **2014,** 760, 24-32.

55. Egami, N.; Hama, A., Dose-Rate Effects on Hatchability of Irradiated Embryos of Fish, Oryzias-Latipes. *Int J Radiat Biol* **1975,** 28, (3), 273-278.

56. Suyama, I.; Etoh, H.; Maruyama, T.; Kato, Y.; Ichikawa, R., Effects of ionizing radiation on the early development of Oryzias eggs. *Journal of radiation research* **1981,** 22, (1), 125-33.

57. Kuwahara, Y.; Shimada, A.; Mitani, H.; Shima, A., A critical stage in spermatogenesis for radiation-induced cell death in the medaka fish, Oryzias latipes. *Radiation research* **2002,** 157, (4), 386-392.

58. Kuwahara, Y.; Shimada, A.; Mitani, H.; Shima, A., gamma-ray exposure accelerates spermatogenesis of medaka fish, Oryzias latipes. *Molecular reproduction and development* **2003,** 65, (2), 204-211.

59. Matsuda, M.; Nagahama, Y.; Shinomiya, A.; Sato, T.; Matsuda, C.; Kobayashi, T.; Morrey, C. E.; Shibata, N.; Asakawa, S.; Shimizu, N.; Hori, H.; Hamaguchi, S.; Sakaizumi, M.,

 doi:10.20944/preprints201908.0002.v1

DMY is a Y-specific DM-domain gene required for male development in the medaka fish. *Nature* **2002,** 417, (6888), 559-563.

60. Nanda, I.; Kondo, M.; Hornung, U.; Asakawa, S.; Winkler, C.; Shimizu, A.; Shan, Z. H.; Haaf, T.; Shimizu, N.; Shima, A.; Schmid, M.; Schartl, M., A duplicated copy of DMRT1 in the sex-determining region of the Y chromosome of the medaka, Oryzias latipes. *Proceedings of the National Academy of Sciences of the United States of America* **2002,** 99, (18), 11778-11783.

61. Saito, D.; Tanaka, M., Comparative Aspects of Gonadal Sex Differentiation in Medaka: A Conserved Role of Developing Oocytes in Sexual Canalization. *Sexual Development* **2009,** 3, (2-3), 99-107.

62. Sato, T.; Endo, T.; Yamahira, K.; Hamaguchi, S.; Sakaizumi, M., Induction of female-to-male sex reversal by high temperature treatment in medaka, Oryzias latipes. *Zool Sci* **2005,** 22, (9), 985-988.

63. Egami, N., Effect of estrogen administration on oviposition of the fish, Oryzias latipes. *Endocrinologia japonica* **1955,** 2, (2), 89-98.

64. Egami, N., Testis-ovum production in starved males. *Jour Fac Sci Tokyo U* **1955,** 7, 421-428.

65. Yamamoto, T., Artificial Induction of Functional Sex-Reversal in Genotypic Females of

 doi:10.20944/preprints201908.0002.v1

the Medaka (Oryzias-Latipes). *Journal of Experimental Zoology* **1958,** 137, (2), 227-&.

66. Shibata, N.; Hamaguchi, S., Evidence for the Sexual Bipotentiality of Spermatogonia in the Fish, Oryzias-Latipes. *Journal of Experimental Zoology* **1988,** 245, (1), 71-77.

67. Gray, M. A.; Niimi, A. J.; Metcalfe, C. D., Factors affecting the development of testis-ova in medaka, Oryzias latipes, exposed to octylphenol. *Environmental Toxicology and Chemistry* **1999,** 18, (8), 1835-1842.

68. Seki, M.; Yokota, H.; Matsubara, H.; Tsuruda, Y.; Maeda, N.; Tadokoro, H.; Kobayashi, K., Effect of ethinylestradiol on the reproduction and induction of vitellogenin and testis-ova in medaka (Oryzias latipes). *Environmental Toxicology and Chemistry* **2002,** 21, (8), 1692-1698.

69. Hirakawa, I.; Miyagawa, S.; Katsu, Y.; Kagami, Y.; Tatarazako, N.; Kobayashi, T.; Kusano, T.; Mizutani, T.; Ogino, Y.; Takeuchi, T.; Ohta, Y.; Iguchi, T., Gene expression profiles in the testis associated with testis-ova in adult Japanese medaka (Oryziaslatipes) exposed to 17alpha-ethinylestradiol. *Chemosphere* **2012,** 87, (7), 668-74.